(6) Allen, N. S.; McKellar, J. F. *Chem. Br.* **1980**, *16*, 480.
(7) Trozzolo, A. M.; Winslow, F. H. *Macromolecules* **1968**, *1*, 98.
(8) Briggs, P. J.; McKeller, J. F. *J. Appl. Polym. Sci.* **1968**, *12*, 1825.
(9) McKeller, J. F.; Allen, N. S. *Photochemistry of Man Made Polymers*; Applied Science: London **1979**.
(10) Carlsson, D. J.; Wiles, D. M. *J. Macromol. Sci., Rev. Macromol. Chem.* **1976**, *C14*, 155.
(11) Allen, N. S.; Homer, J.; McKeller, J. F. *Makromol. Chem.* **1978**, *179*, 1575.
(12) Allen, N. S.; McKeller, J. F. *Chem. Soc. Rev.* **1975**, *4*, 553.
(13) Stewart, L. C.; Carlsson, D. J.; Wiles, D. M.; Scaiano, J. C. *J. Am. Chem. Soc.* **1983**, *105*, 3605.
(14) Bortolus, P.; Dellonte, S.; Faucitano, A.; Gratani, F. *Macromolecules* **1986**, *19*, 2916.
(15) Schirmann, P. J. *ACS Symp. Ser.* **1987**, 870.
(16) Emanuel, N. M.; Buchachenko, A. L. *Chemical Physics of Polymer Degradation and Stabilization*; C.R.N.I. de Jonge: Utrecht, 1987.
(17) Elbs, K.; Keiper, W. *J. Prakt. Chem.* **1905**, *67*, 580.
(18) Monte, D. D.; Mangini, A.; Passerini, R.; Zauli, C. *Gazz. Chim. Ital.* **1958**, *88*, 977.
(19) Belusa, J.; Janousek, Z.; Knovlickova, H. *Chem. Zvesti* **1974**, *28*, 673.
(20) Heller, H.; Rody, J.; Keller, E. U.S. Patent 3 399 173, 1968; *Chem. Abstr.* **1968**, *69*, 87597W.
(21) Yoshida, S.; Volg, O. *Polym. Prepr. (Am. Chem. Soc., Div. Polym. Chem.)* **1980**, *21*, 203.
(22) Pradellok, W.; Vogl, O. *J. Polym. Sci., Polym. Chem. Ed.* **1981**, *19*, 3307.
(23) Nir, Z.; Vogl, O. *J. Polym. Sci., Polym. Chem. Ed.* **1982**, *20*, 2735.
(24) Yoshida, S.; Vogl, O. *Makromol. Chem.* **1982**, *183*, 259.
(25) Yoshida, S.; Lillya, C. P.; Vogl, O. *J. Polym. Sci., Polym. Chem. Ed.* **1982**, *20*, 2215.
(26) Li, S.; Bassett, W.; Gupta, A.; Vogl, O. *J. Macromol. Sci., Chem.* **1983**, *A20* (3), 309.
(27) Xi, F.; Bassett, W.; Vogl, O. *Makromol. Chem.* **1984**, *185*, 2497.
(28) Vogl, O.; Albertsson, A. C.; Janovic, Z. *Polymer* **1985**, *26*, 1288.
(29) Dickstein, W.; Vogl, O. *J. Macromol. Sci., Chem.* **1985**, *A22* (4), 387.
(30) Gupta, A.; Sarbolouki, M. N.; Huston, A. C.; Scott, G. W.; Pradellok, W.; Vogl, O. *J. Macromol. Sci., Chem.* **1986**, *A23* (10), 1179.
(31) Borsig, E.; Gupta, A.; Rånby, B.; Vogl, O. *Polym. Bull.* **1984**, *12* (3), 245.
(32) Recca, A.; Libertini, E.; Finocchiaro, P.; Munro, H. S.; Clark, D. T. *Macromolecules* **1988**, *21*, 2641.
(33) Munro, H. S.; Banks, J.; Recca, A.; Bottino, F. A.; Pollicino, A. *Polym. Degrad. Stab.* **1986**, *15*, 161.
(34) Munro, H. S.; Banks, J.; Bottino, F. A.; Pollicino, A.; Recca, A. *Polym. Degrad. Stab.* **1987**, *17*, 185.
(35) Munro, H. S.; Bottino, F. A.; Pollicino, A.; Recca, A. *Polym. Degr. Stab.* **1988**, *23*, 19.
(36) Briggs, D. In *Practical surface analysis*; Briggs, D., Seah, M. P., Eds.; Wiley: Chichester **1983**.
(37) Hodgeman, D. K. C. *J. Polym. Sci., Polym. Lett. Ed.* **1978**, 16, 161.
(38) Sasson, Y.; Yonovich, M. *Tetrahedron Lett.* **1979**, *39*, 3753.
(39) Schosser, M.; Schaub, B. *Chimia 36* **1982**, *10*, 396.
(40) Munro, H. S. *Polym. Degrad. Stab.* **1985**, *12*, 249.
(41) Clark, D. T.; Munro, H. S. *Polym. Degrad. Stab.* **1984**, *8*, 195.

Registry No. 1, 104585-00-4; 1 (homopolymer), 116803-05-5; **1a**, 114505-27-0; **1b**, 114505-28-1; **2**, 125846-37-9; **2a**, 27959-42-8; **2a'**, 125846-38-0; **2b**, 125846-34-6; **3**, 77865-92-0; **3a**, 125846-33-5; **3b**, 125846-35-7; **4**, 83739-91-7; **4a**, 93525-19-0; **4b**, 125846-36-8; methyltriphenylphosphonium bromide, 1779-49-3; sodium amide, 7782-92-5.

Excimer Formation in Sterically Hindered Poly(9-vinylcarbazole) and Its Dimer Model Compounds

Shinzaburo Ito, Kazukiyo Takami, Yoshinobu Tsujii, and Masahide Yamamoto*

Department of Polymer Chemistry, Faculty of Engineering, Kyoto University, Sakyo-ku, Kyoto 606, Japan

Received July 5, 1989; Revised Manuscript Received October 27, 1989

ABSTRACT: The fluorescence properties, especially the excimer formation process, in poly(3,6-di-*tert*-butyl-9-vinylcarbazole) (PBVCz) and its dimeric model compounds, *meso*- and *rac*-2,4-bis(3,6-di-*tert*-butyl-9-carbazolyl)pentanes (*meso*- and *rac*-BCzPe), have been investigated. The molecular structure of poly(9-vinylcarbazole) (PVCz) was modified by bulky *tert*-butyl substituents on the carbazole ring. PBVCz and *rac*-BCzPe show broad excimer emission at wavelengths slightly shifted from the excited monomer band. Since sandwich excimer formation is hindered by the bulky groups, this polymer exhibits a unique excimer formed by the syndiotactic diads. To investigate the excimer formation process, ^{1}H NMR analysis and calculation of conformational energies were carried out for *rac*-BCzPe. The result indicates that a partially overlapping arrangement of the carbazole rings is attained by parallel rotation of two aromatic planes from the stable TT conformation, but the extent of overlapping is quite small. These data show that the carbazole excimer has fairly continuous energy levels, depending on the degree of overlapping of the aromatic planes.

Introduction

The excimer formation mechanism in poly(9-vinylcarbazole) (PVCz) has attracted much attention in the field of polymer photophysics. At least two kinds of excimers are known, the fully overlapped excimer (sandwich excimer) and the partially overlapped excimer (second excimer), besides the excited monomer state.[1,2] Since these two kinds of excimer emissions were found in PVCz, extensive kinetic studies have been carried out by using various dimeric model compounds.[3-6] The meso and racemic isomers of 2,4-disubstituted pentanes are good models for the isotactic and the syndiotactic diads in the polymer chain, respectively. The advantage of using model compounds is that quantitative studies can be conducted based on a simple kinetic scheme involving estab-

0024-9297/90/2223-2666$02.50/0 © 1990 American Chemical Society

lished molecular structures. Recent developments in the time-resolved technique for fluorescence measurements have revealed the excimer formation kinetics in the pentane dimers. However, the complicated nature of PVCz has been extensively discussed,[7-11] and various kinetic models have been proposed. To interpret the nonexponential decay curves of the monomer and the second excimer emission, some workers assumed the existence of several kinds of excited intermediates[12] or proposed a nonexponential trapping process of the excitation energy.[13,14]

Besides the kinetic studies with time-resolved measurements, one effective approach to photophysical problems is structure modification of the chromophoric compounds. The well-known Hirayama $n = 3$ rule is typical of the fruit of such structural studies.[15] With respect to polymers containing the carbazole chromophore, Ledwith et al. synthesized poly(vinylcarbazoles) in which the vinyl group is substituted at different positions of the carbazole ring and reported significant differences in their excimer kinetics.[16] Houben et al. also prepared a series of poly(vinylcarbazoles) having a bulky substituent, which effectively reduces excimer formation efficiency.[17] Polymer samples in which the carbazole chromophore is attached to the main chain with some spacer atoms show quite different photophysical behavior.[18-22] This type of structural arrangement weakens the interaction between carbazole chromophores and makes the excited species much simpler than those of PVCz. Thus, the peculiar characteristics of PVCz have been revealed by these structural investigations.

Recently, we synthesized a new polymer, poly(3,6-di-*tert*-butyl-9-vinylcarbazole), and its dimeric model compounds. The bulky substituents on the carbazole ring

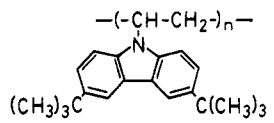

PBVCz

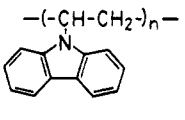

PVCz

are expected to hinder excimer formation and to simplify the kinetic scheme in the excited states. Conformational restriction by the bulky groups seems to give further information on the geometrical arrangement of the carbazole rings in the excimer form. In a previous communication, we briefly reported the fluorescence properties and showed that a high-energy excimer is formed despite the bulky groups.[23] In the current study, ^{1}H NMR analysis and empirical calculation of conformational energies are applied to the dimer models, and the steric effect of the substituents on the excimer kinetics is clarified, compared with the model compounds of PVCz.

Experimental Section

Materials. 3,6-Di-*tert*-butylcarbazole (BCz). Carbazole (Tokyo Chemical Industry Co., Ltd.) and *tert*-butyl chloride were allowed to react in the presence of aluminum chloride.[24,25] The crude product was distilled twice under reduced pressure. After distillation of carbazole and monosubstituted carbazole, BCz was obtained as a viscous oil: 180 °C at 3 Torr. Repeated recrystallization from hexane solution gave white needles: mp 223 °C.

3,6-Di-*tert*-butyl-9-ethylcarbazole (BEtCz). To a THF solution of sodium 3,6-di-*tert*-butylcarbazole, an equimolar amount of bromoethane was added dropwise, and the mixture was refluxed for 3 h. After extraction with benzene, the crude product was purified by column chromatography on silica gel with a mixed solvent of hexane and benzene (4:1) as eluent: mp 153–154 °C; IR (KBr) 2970, 2900, 2870, 1480, 1380, 1300, 1160, 810 cm^{-1}; ^{1}H NMR ($CDCl_3$) δ 1.40 (t, 3 H), 1.45 (s, 18 H), 4.31 (q, 2 H), 7.20–7.65 (m, 4 H), 8.09 (s, 2 H).

2,4-Bis(3,6-di-*tert*-butyl-9-carbazolyl)pentane (BCzPe). To a solution of BCz (3 g) in dried DMF, 0.5 g of sodium hydride was added. The mixture was heated for 1 h at 60 °C and then cooled to room temperature. A DMF solution of 2,4-bis(tosyloxy)pentane (2.2 g) was added dropwise. After heating for 1 h at 60 °C, the solution was extracted several times with dichloromethane and water. The crude product was purified by column chromatography on silica gel with a mixed solvent of hexane and benzene (9:1) as eluent. Thus obtained BCzPe was separated into the racemic and meso isomers by liquid chromatography (Japan Spectroscopic Co., Ltd.) with a mixture of hexane and ethyl acetate (100:1) as eluent: IR (KBr) 2950, 2850, 1490, 1360, 1300, 800 cm^{-1}; ^{1}H NMR for *rac*-BCzPe ($CDCl_3$) δ 1.448 (d, 6 H, methyl), 1.452 (s, 36 H, *tert*-butyl), 3.05 (m, 2 H), 4.51 (m, 2 H), 6.1–6.6 (br, 2 H), 6.9–7.8 (br, 6 H), 8.10 (s, 4 H); ^{1}H NMR for *meso*-BCzPe δ 1.45 (s, 36 H), 1.63 (d, 6 H), 2.89 (m, 2 H), 4.56 (m, 2 H), 6.8–7.4 (br, 8 H), 8.06 (s, 4 H).

Poly(3,6-di-*tert*-butyl-9-vinylcarbazole) (PBVCz). By the reaction of BCz with (2-chloroethyl)-*p*-toluenesulfonate, 9-(2-chloroethyl)-3,6-di-*tert*-butylcarbazole was obtained and purified by recrystallization from methanol and by column chromatography on silica gel. To an ethanol solution (25 mL) of this product (0.8 g), a methanol solution of potassium hydroxide (6 g) was added. The mixture was refluxed for 3 h and poured into ice water. The precipitate was washed with water. After three recrystallizations from methanol white crystalline 3,6-di-*tert*-butyl-9-vinylcarbazole (BVCz) was obtained: mp 74 °C; IR (KBr) 2960, 2900, 2860, 1640, 1480, 1360, 1300, 800 cm^{-1}; ^{1}H NMR (benzene-d_6) δ 1.44 (d, 18 H), 4.80 (d, 1 H), 5.36 (d, 1 H), 7.10 (q, 1 H), 7.45 (s, 4 H), 8.22 (s, 2 H). The BVCz was polymerized in dichloromethane at −78 °C, using boron trifluoride diethyl etherate as an initiator. The PBVCz obtained was purified by repeated reprecipitation from dichloromethane solution into methanol. The molecular weight was determined by GPC (TOSOH HLC 802UR) to be 10^6 on the basis of a calibration with polystyrene standards. This polymer was found to be mainly syndiotactic from the similarity of the methine signal to that of PVCz in the ^{1}H NMR spectra.[26]

Poly(9-vinylcarbazole) (PVCz). 9-Vinylcarbazole (Tokyo Chemical Industry Co., Ltd.) was purified by recrystallization from ethanol and hexane and polymerized in the same manner as PBVCz.

2-Methyltetrahydrofuran (MTHF). Purchased MTHF (Nacalai Tesque, Inc.) was purified by an alumina column, distillation over sodium metal, and finally vacuum distillation before use.

Measurements. Spectroscopic measurements were carried out in deaerated MTHF solutions; the concentration of carbazole chromophore was adjusted to ca. 2×10^{-5} mol L^{-1}, where the reabsorption effect on the fluorescence spectra and decay measurements can be ignored. Absorption spectra were recorded with a Shimadzu UV-200S spectrophotometer. Fluorescence spectra were measured with a Hitachi 850 spectrofluorophotometer in which the spectral response was corrected. The quantum yields of emission were determined relative to that of quinine sulfate in 0.5 mol L^{-1} sulfuric acid.[27]

The decay curves and time-resolved fluorescence spectra were measured by a single-photon-counting method. The pulsed excitation light was obtained with a Spectra-Physics picosecond synchronously pumped mode-locked cavity dumped dye laser (Model 2020, 342A, 375B, 344S). The emission from the samples was detected with a microchannel plate photomultiplier (Hamamatsu R1564U-01).[28] The signals obtained by Ortec photon-counting electronics were accumulated on a multichannel analyzer (Norland IT-5300) controlled with a microcomputer (NEC PC9801). The fwhm of the overall excitation pulse was 75 ps. The decay data were deconvoluted by fitting to theoretical functions using a nonlinear least-squares fitting program. The quality of fit was judged by the reduced χ^2 criterion.

NMR spectra were measured with a JEOL GX-400 400-MHz spectrometer and with a JEOL FX-90Q 90-MHz spectrometer. Tetramethylsilane was used as an internal reference.

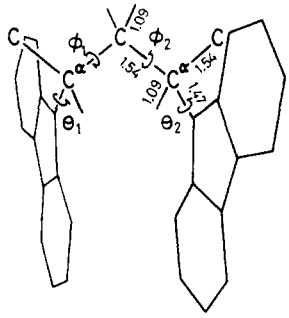

Figure 1. Structural parameters of racemic dimers used for conformational analysis.

Calculation of Conformational Energy. The conformational energies of *rac*-BCzPe and *rac*-CzPe were calculated by the conventional empirical method described in the preceding papers.[29,30] The total potential energies were given by the sum of the van der Waals interactions between nonbonded atoms, the intrinsic torsional potentials of skeletal C–C bonds, and the dipole–dipole interaction between two carbazole chromophores. For calculation of the van der Waals energies, a Lennard-Jones type function was employed, in which the function was truncated by considering the molecule–solvent interaction according to Flory et al.[31] The torsional energies were calculated for the rotational angles of an alkane chain with a threefold periodicity, in which the torsional barrier energy was taken to be 2.8 kcal mol^{-1}.[31] The torsional energies for the rotation of carbazole rings was neglected, since the potential barrier is known to be too low. The dipole moment of the carbazole ring was taken to be 2.09 D along the C^α–N bonds,[32] and the dielectric constant of the solvent was 6.24 for MTHF at 25 °C.[33] Figure 1 shows the structural parameters used in this calculation. Four independent rotational angles are needed to generate a given conformation of BCzPe: two rotational angles ϕ_1 and ϕ_2 for the alkane chain, and two angles θ_1 and θ_2 for the carbazole ring, which are denoted in Figure 1. The angles ϕ were taken as 0° in the trans conformation, and the angles θ were 0° when the aromatic plane became coplanar to the neighboring methine proton. The structural parameters for the carbazole ring were obtained from X-ray data of carbazole derivatives.[34,35] According to Sundararajan, the bond angle of the alkane chain used was $\angle CC^\alpha C = 112°$, and the angle $\angle C^\alpha CC^\alpha$ was varied from 110° to 122° since the angle at the methylene carbon tends to become large with the size of the side groups and with the conformation of the dimeric unit.[36]

Results and Discussion

Fluorescence Spectra. Figure 2 shows the fluorescence spectra of PBVCz, BCzPe, and BEtCz at 25 °C. BEtCz is regarded as a monomeric model compound and gives monomer fluorescence from an isolated BCz chromophore. The S_1–S_0 band appears at 360 nm, which is shifted ca. 10 nm longer than the band of 9-ethylcarbazole. This shift is attributed to the effect of alkyl substitution on the carbazole ring at the 3,6-position. *meso*-BCzPe shows neither the sandwich excimer nor the second excimer fluorescence. This is notably different from the behavior of other kinds of meso dimers: e.g., corresponding meso dimers having phenyl, naphthyl, and pyrenyl chromophores show efficient excimer formation, and *meso*-2,4-bis(9-carbazolyl)pentane (*meso*-CzPe) is known to form the sandwich excimer with a high quantum efficiency.[5,6] Thus, the bulky *tert*-butyl groups completely prevent the overlapping of carbazole rings.

On the other hand, PBVCz and *rac*-BCzPe show excimer emission. Broad excimeric emission can be observed near the second vibration band of the monomer fluorescence (maximum wavelength: 372 nm). This emission is quite similar to the second excimer observed in PVCz, but the spectral shift from the monomer fluorescence band

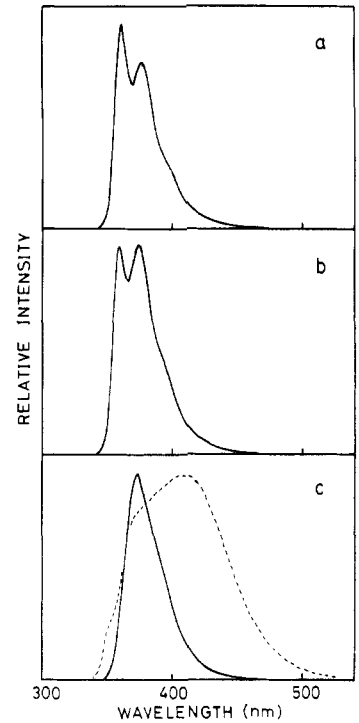

Figure 2. Fluorescence spectra of (a) BEtCz and *meso*-BCzPe, (b) *rac*-BCzPe, and (c) PBVCz in MTHF at 25 °C. The broken line is the spectrum of PVCz under the same conditions. The excitation wavelength is 330 nm. Spectra are recorded with a bandwidth of 2 nm and normalized to the same intensity at the maximum.

is much smaller than that of PVCz: 900 cm^{-1} for PBVCz and 1740 cm^{-1} for PVCz. This means that the stabilization energy of the PBVCz excimer is smaller than that of the second excimer of PVCz since the overlapping of the carbazole rings is insufficient due to the large steric hindrance. The excimer emission has a narrow bandwidth and no tail in the longer wavelength region. As mentioned for *meso*-BCzPe, this polymer is also prevented from forming a sandwich excimer, which would appear at ca. 420 nm. For comparison, the spectrum of PVCz is shown by a broken line in Figure 2c.

rac-BCzPe gives both monomer and excimer emission. The fractions of monomer and excimer emission at 25 °C are ca. 0.7 and 0.3, respectively. This ratio changes upon decrease of temperature, as shown in Figure 3. At temperatures below −100 °C, the spectra consist only of the monomer fluorescence. This fact indicates that excimer formation in *rac*-BCzPe occurs by some dynamic processes, e.g., conformational rearrangement after the excitation. On the other hand, the fluorescence spectra of PBVCz did not change over a wide temperature range. Even at 77 K, the spectrum gives excimer emission similar to that in Figure 2, and no vibrational bands from monomer emission are observed. These results indicate that the carbazole chromophore in syndiotactic diads in the polymer chain forms a partially overlapping excimer site with a high probability, and efficient energy migration occurs rapidly to this site. It is noteworthy that this polymer forms no sandwich excimer, which would act as a deep trap of excitation energy.

Time-Resolved Measurements. Figure 4 shows time-resolved fluorescence spectra PBVCz and *rac*-BCzPe at 25 °C. The excimer formation process in PBVCz (Figure 4b) is already over within 100 ps after excitation, and no spectral change is observed at any observation time under the available time resolution. In the measurement at 77 K, weak monomer emission rapidly decays

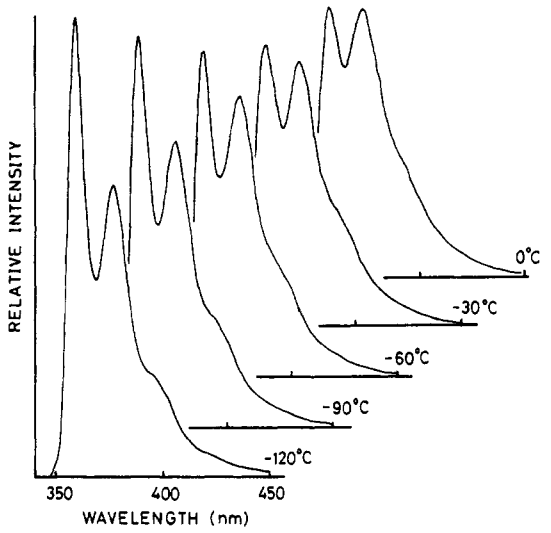

Figure 3. Temperature dependence of fluorescence spectra of *rac*-BCzPe. The excitation and the bandwidth are the same as those in Figure 2.

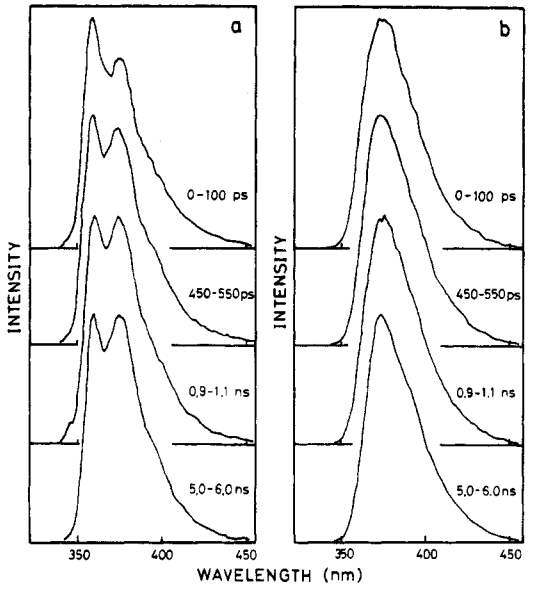

Figure 4. Time-resolved fluorescence spectra of (a) *rac*-BCzPe and (b) PBVCz at 25 °C. The excitation wavelength is 300 nm and the bandwidths are (a) 2 nm and (b) 4 nm. Spectra are normalized to the same maximum intensity. Numerals show the observation times after the time of maximum intensity of the excitation pulse.

immediately after the excitation. These facts show that the excimer formation rate, which probably corresponds to the rate of energy migration to the excimer sites, is $>10^{10}$ s^{-1}.

rac-BCzPe shows the spectral change shortly after excitation (Figure 4a). The monomer band at 360 nm clearly decreases with time at the early stage. Thereafter, the spectra decay with the ratio of the monomer emission to the excimer emission kept constant. This means that interconversion between the monomer and the excimer states reaches equilibrium within a few nanoseconds.

We tried to determine the excimer formation and dissociation rate constants of *rac*-BCzPe by decay measurements. Fluorescence decay curves were measured at various wavelengths, and observed data were fitted by the sum of two or three exponential functions. A good fit was obtained with two exponentials as shown in Figure 5, and no improvement in fit was found for the sum of three exponential functions. Here, there is an experimental difficulty in this system. As shown in Figure 2,

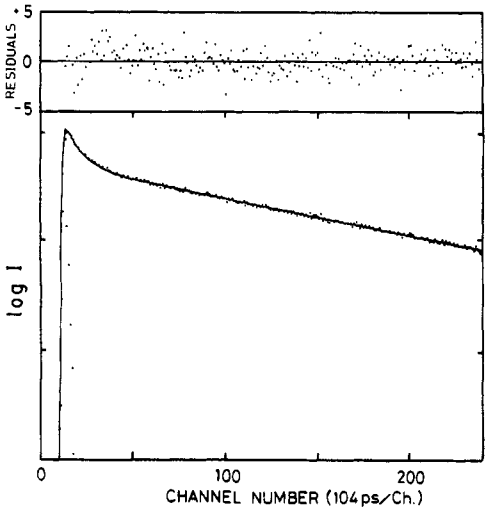

Figure 5. Fluorescence decay curve of *rac*-BCzPe observed at 350 nm. The excitation wavelength is 300 nm. The solid line is a best-fit curve for the parameters: $\lambda_1^{-1} = 13.3$ ns, $\lambda_2^{-1} = 0.86$ ns, $A = 1.44$, $\chi^2 = 1.36$.

the excimer emission has a narrow bandwidth compared to that of the second or sandwich excimer. It appears within the wavelength region of the monomer fluorescence, so we could not separately observe the monomer and excimer fluorescence decays. At 350 nm (the leading edge of the monomer fluorescence), a clear two-component decay curve is obtained, but the fraction of the fast component changes with the observed wavelengths. This means that the observed decay curve is a sum of the monomer and excimer decays. Since the quantum yield of excimer is about half that of the monomer emission and since the excimer spectrum showed no tail at long wavelengths, a rise of excimer is not observed at any wavelengths behind the monomer emission. Under such conditions, the fractions obtained from the decay parameters are not useful but the time constants have an important meaning. The decay curves at 350, 358, 372, and 390 nm are fitted with the same two time constants listed in Table I. The excitation spectrum monitored at 372 nm (the wavelength for the maximum intensity of excimer emission) is the same as that at 360 nm. Furthermore, as shown in Figure 3, the temperature dependence of the fluorescence spectra indicates that the excimer is formed by dynamic processes after excitation. On the basis of these facts, the conventional Birks kinetics was employed as follows.[37]

$$\mathrm{M}^* \rightarrow \mathrm{M} + h\nu_1 \quad k_{01}^{\mathrm{f}}$$

$$\mathrm{M}^* \rightarrow \mathrm{M} \quad k_{01}^{\mathrm{n}}$$

$$\mathrm{M}^* \rightarrow \mathrm{D}^* \quad k_{21}$$

$$\mathrm{D}^* \rightarrow \mathrm{M}^* \quad k_{12}$$

$$\mathrm{D}^* \rightarrow \mathrm{M} + h\nu_2 \quad k_{02}^{\mathrm{f}}$$

$$\mathrm{D}^* \rightarrow \mathrm{M} \quad k_{02}^{\mathrm{n}}$$

M and M* represent the BCz chromophore in the ground state and the excited monomer state, respectively, and D* is the intramolecular excimer. Under this kinetic scheme, the decay curves of the monomer and the excimer fluorescence are represented as follows.

$$I_{\mathrm{M}}(t) = \exp(-\lambda_1 t) + A \exp(-\lambda_2 t)$$

$$I_{\mathrm{D}}(t) = \exp(-\lambda_1 t) - \exp(-\lambda_2 t)$$

A is a constant and λ_1 and λ_2 are given as functions of

Table I
Observed Quantum Yields, Decay Rates, and Calculated Rate Constants

	Φ_M	Φ_D	λ_1, 10^7 s^{-1}	λ_2, 10^7 s^{-1}	k_{01}^f, 10^7 s^{-1}	k_{01}^n, 10^7 s^{-1}	k_{21}, 10^7 s^{-1}	k_{12}, 10^7 s^{-1}
BEtCz	0.445		7.35		3.27	4.08		
rac-BCzPe	0.318	0.129	7.53	116	3.27[a]	4.08[a]	31	77

[a] Values estimated from the data of BEtCz.

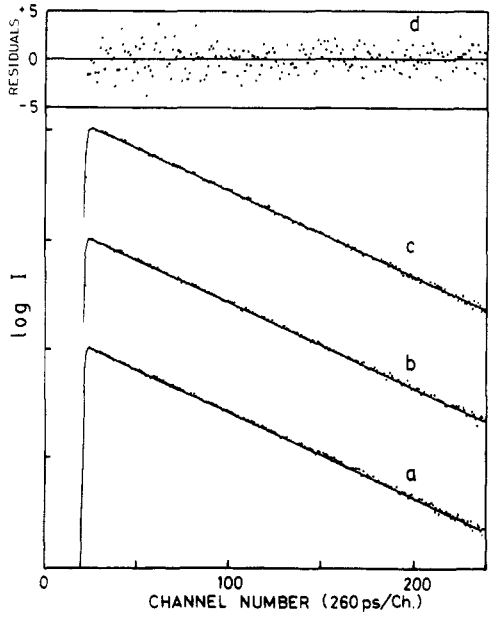

Figure 6. Fluorescence decay curves of PBVCz at (a) 372 nm, (b) 390 nm, and (c) 420 nm. Solid lines are the curves calculated from a single-exponential function with a lifetime of 14.4 ± 0.2 ns. The plot (d) shows the weighted residuals for the decay curve at 372 nm.

rate constants.[37] λ_1 and λ_2 are obtained as the best-fit parameters of the decay curves. Other observable values are the quantum yields of the monomer and the excimer fluorescence, Φ_M and Φ_D, respectively. These values are represented by the following relations.

$$\Phi_M = k_{01}^f(k_{02}^f + k_{02}^n + k_{12})/\lambda_1\lambda_2$$

$$\Phi_D = k_{02}^f k_{21}/\lambda_1\lambda_2$$

$$\lambda_1 + \lambda_2 = k_{01}^f + k_{01}^n + k_{21} + k_{02}^f + k_{02}^n + k_{12}$$

$$\lambda_1\lambda_2 = (k_{01}^f + k_{01}^n + k_{21})(k_{02}^f + k_{02}^n + k_{12}) - k_{21}k_{12}$$

The rate constants k_{01}^f and k_{01}^n are determined by the measurement of the quantum yield and the lifetime of BEtCz; then the other four rate constants can be obtained by using the above equations. Table I shows the results. Instability of this excimer is represented as the slow formation rate and fast dissociation rate constants.

The excimer formation rate of PBVCz is too fast to be determined by time-resolved measurements. Observed decay curves at various wavelengths are the same and are represented with a single-exponential function. Figure 6 shows the best-fit curves, which are the same exponential function with the lifetime of 14.4 ± 0.2 ns. This means that there is only one excited species in the broad excimeric emission. It is well-known that the fluorescence decay curve of PVCz depends on the observed wavelengths and should be fitted with multiexponential or nonexponential functions that reflect the complicated kinetic scheme for PVCz. The bulky groups of PBVCz prevent sandwich excimer formation and simplify the kinetic scheme by a reduction of the number of conformations sterically allowed.

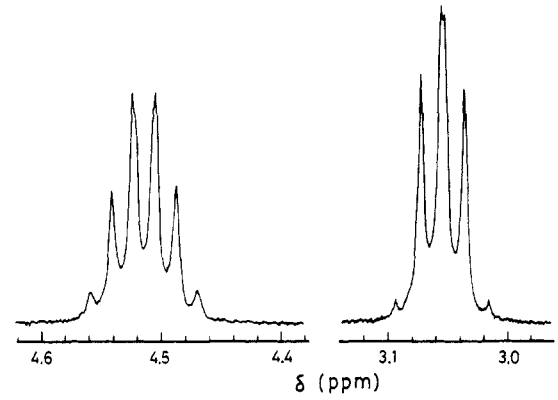

Figure 7. ^{1}H NMR spectra (400 MHz) of the methine (left) and methylene (right) protons of *rac*-BCzPe in $CDCl_3$ at 30 °C.

Stable Conformation of Racemic Dimer. It is very important to know the ground-state conformations of *rac*-BCzPe, which are the starting points of conformational rearrangement to the excimer form. The ^{1}H NMR data for *rac*-CzPe have already been reported.[5,6] The results indicate that the main conformers are the TT and the GG forms, and the fraction of the TT form is estimated to be 0.9 at room temperature. To examine the substitution effect on the ground-state conformation, ^{1}H NMR data were analyzed according to Bovey[38] and Abe et al.[39] Figure 7 shows the methine and methylene proton spectra of *rac*-BCzPe, which were analyzed by using the LAOCOON III program, assuming an AA′XX′ spin system. The best-fit values of the vicinal coupling constants, J_{AX} and $J_{AX'}$, and the geminal coupling constant, $J_{AA'}$, are as follows: J_{AX} = 9.36 Hz, $J_{AX'}$ = 5.15 Hz, and $J_{AA'}$ = −15.22 Hz.

Under the condition that the high-energy conformations can be ignored, that is, the conformers are predominantly in the TT and the GG forms, J_{AX} and $J_{AX'}$ are given by

$$J_{AX} = f_{TT}J_T + f_{GG}J_G$$

$$J_{AX'} = f_{TT}J_G + f_{GG}J_T$$

Here, f_{TT} and f_{GG} are the fractions of the TT and the GG conformers, respectively. To obtain f_{TT} and f_{GG} values, it is necessary to assume the constants for trans coupling, J_T, and the gauche coupling, J_G. Abe et al. adopted the ratio J_G/J_T = 0.307 on the basis of the data for some cyclic model compounds.[39] With this value and the observed J_{AX} and $J_{AX'}$ values, the conformer population was calculated as follows.

$$f_{TT} = 0.77 \quad (f_{GG} = 0.23)$$

As mentioned above, De Schryver et al. reported that f_{TT} for *rac*-CzPe is 0.885 at 298 K in octane,[5] and Abe et al. estimated it to be 0.86 for the simplest condition that the fractions of high-energy conformers are negligibly small.[39] The result for *rac*-BCzPe clearly indicates that the population of the TT form is somewhat smaller than that for *rac*-CzPe, but the main conformer is still the TT form, in spite of the substitution of the large *tert*-butyl groups on the carbazole chromophore.

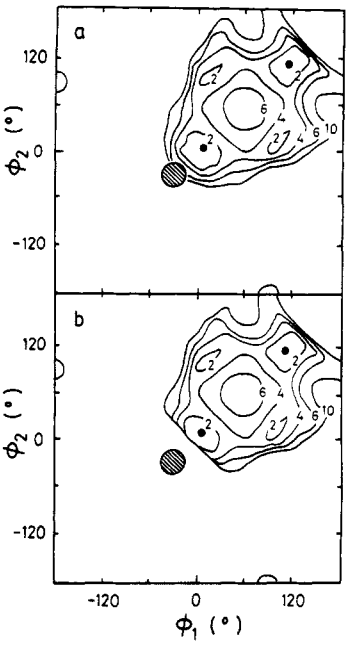

Figure 8. Conformational energy maps of (a) *rac*-CzPe and (b) *rac*-BCzPe. Numerals on the contours are the values of the energies (kcal mol^{-1}) relative to the minimum energy at the position marked by a filled circle. The shaded circles represent the position for the second excimer conformation.

Calculation of Conformational Energy. The ^{1}H NMR data show that a large portion of *rac*-BCzPe assumes a TT conformation in the ground state and just when the carbazole chromophore is excited. The next problem is the pathway to the excimer and the geometrical arrangement of the excimer. To obtain further insight into this problem, we carried out the calculation of conformational energies. Unfortunately, our knowledge is still insufficient to calculate the exact interaction energies between excited chromophores in various geometrical arrangements. At the present stage, a conventional empirical method for ground-state molecules is employed. This calculation is expected to give information on the particular arrangements in which the van der Waals repulsion force becomes too large. Even if some attractive forces act between a pair of chromophores in the excited state, it is impossible to overcome a repulsive potential of a few tens of kcal mol^{-1} caused by the interaction between alkyl substituents and other atoms that do not belong to the π-electron system.

First, potential energies of *rac*-BCzPe and *rac*-CzPe were calculated for the skeletal bond rotations. Figure 8 shows the energy map as a function of ϕ_1 and ϕ_2, where the angles θ_1 and θ_2 are fixed at 0°. In this figure, the minimum is marked by a filled circle. The shaded part is the second excimer position proposed for *rac*-CzPe by Itaya et al.[2] This position is one of the unstable conformations in the ground state but is stabilized in the excited state by the electronic interaction between carbazole chromophores. The positions (0°, 0°) and (120°, 120°) represent the TT and the GG forms, respectively, but the minima appeared around (5–10°, 5–10°) and (110–115°, 110–115°) for both compounds. The lowest energy on the map appears at the TT form or the GG form, depending on the value of $\angle C^{\alpha}CC^{\alpha}$. The calculated minimum energies at the TT and the GG forms are not much different. The TT form corresponds to the planar trans conformation of the alkane chain, and it is near the excimer conformation. On the whole, the two energy maps are similar. This agrees with the NMR data mentioned above.

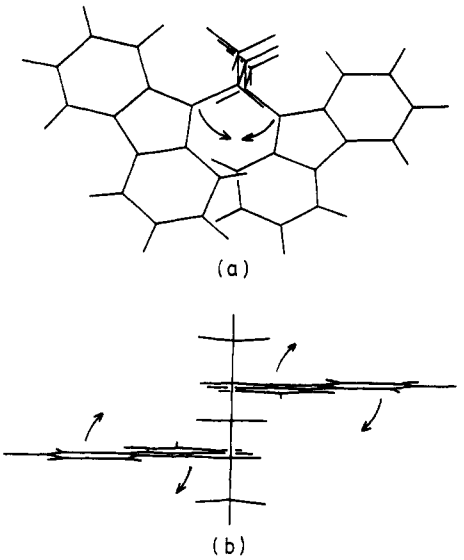

Figure 9. Schematic illustration of conformational movements to the excimer form: (a) symmetrical rotation of ϕ; (b) parallel rotation of θ.

A marked difference in the maps between *rac*-BCzPe and *rac*-CzPe is seen in the part near the TT conformation. The potential energy for *rac*-BCzPe steeply increases with the conformational change in the direction to the excimer form. The motion on the diagonal line from TT to the lower left part represents the symmetrical approach of the carbazole rings. The *tert*-butyl substituents effectively inhibit this pathway, which would be a most likely motion to the second excimer formation.

To discuss in more detail the pathway of the excimer formation, let us consider two types of combined motions around the TT form, as shown in Figure 9: symmetrical motion of the carbazole rings by rotation of ϕ_1 and ϕ_2 in which $\phi_1 = \phi_2 = \phi$ (Figure 9a), and parallel rotational motion of two aromatic planes where $\theta_1 = \theta_2 = \theta$ (Figure 9b). By the former motion, two chromophores can approach each other with the least increase of intrinsic torsional energy. In the latter motion, the condition of θ is necessary to avoid undesirable collision of large aromatic planes. These two kinds of motions seem to be most probable and easy ways to attain an effective overlapping of the π-electron clouds on the chromophore, which is essential for excimer formation in the excited state.

Figure 10 shows the energy maps for these motions, where the increase of potential energies is drawn by 2-dimensional maps as a function of ϕ and θ. The position of the second excimer assumed for *rac*-CzPe is also indicated by the shaded domain; there is some uncertainty in the size and the center of the shaded circle, but the proposed structure of the second excimer corresponds to the position (ϕ, θ) = (-30°, 0°). The map for *rac*-CzPe has a long valley extending in the direction of the excimer site, but for *rac*-BCzPe, this valley is cut off at the angle $\phi = -5°$ due to the large steric hindrance of the *tert*-butyl groups. This means that overlapping of carbazole rings is impossible only through the rotation of the skeletal C–C bonds. With respect to the high-energy part, a shallow valley is found in the left lower part of the energy map. The situation is explained in Figure 10c, in which the numerals show the distance between the central carbon atoms of the neighboring pair of *tert*-butyl groups. According to the empirical data, the van der Waals radius of *tert*-butyl groups is known to be ca. 0.3 nm. When the distance becomes shorter than 0.6 nm, the conformation is subject to large steric hindrance. The motion corresponding to the valley in

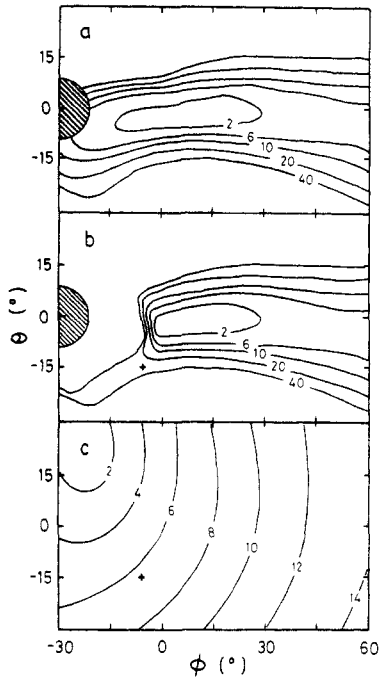

Figure 10. Conformational energy maps of (a) *rac*-CzPe and (b) *rac*-BCzPe around the TT form. The shaded circles represent the second excimer conformation for *rac*-CzPe. In the map (c) the numerals show the distance (Å) between a neighboring pair of *tert*-butyl groups attached to the different carbazole rings. The cross represents the conformation illustrated in Figure 11.

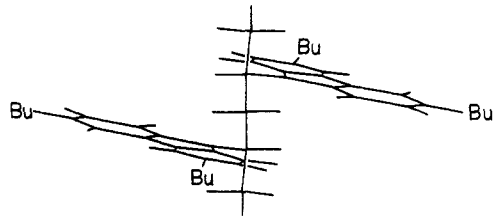

Figure 11. Schematic illustration of the excimer conformation proposed for *rac*-BCzPe. Bu = *tert*-butyl substituent.

Figure 10b satisfies this steric requirement. Furthermore, some overlapping of the carbazole rings becomes possible with this rotation as shown in Figure 11. On the basis of this result, we propose a new partially overlapped excimer formed by parallel rotation of the aromatic planes around the N–C^{α} bonds. Figure 11 is a schematic figure of the conformation at $(\phi, \theta) = (-6°, -15°)$; the position is marked in Figure 10b by a cross.

A disadvantage of this proposal is the high potential energy even at the position marked by the cross. This high energy mainly comes from the interaction between the methylene proton of the alkane chain and the aromatic proton attached to the 1- or 8-position of the carbazole ring. If the distance can be set to a value 0.01 nm longer than the present one, the energy will be reduced to about half its initial potential. Our calculation is based on a "rigid molecule", in which structural parameters are fixed except for the five variable angles; all bond lengths and all bond angles except for $\angle C^{\alpha}CC^{\alpha}$ are fixed. The assumption of a "flexible molecule" will lower the energy by slight adjustments of the molecular parameters. Under the large attractive force in the excited state, the conformation shown in Figure 11 is attainable.

Conclusion

The bulky *tert*-butyl substituents completely prevent sandwich excimer formation both in PBVCz and *meso*-BCzPe. Consequently, PBVCz and *rac*-BCzPe form a unique excimer with a slightly overlapping arrangement of carbazole chromophores. This conformation is probably attained by a parallel rotation of two aromatic planes from the stable TT conformation. Even with such a small extent of overlapping, the excited-state interaction is strong enough to change the spectrum to an excimeric one. This fact shows the characteristic property of the carbazole chromophore, i.e., that the excited state is readily stabilized by interaction with the neighboring chromophore even if there is little overlapping of the aromatic planes.

Acknowledgment. We express our thanks to Prof. I. Yamazaki and Dr. N. Tamai of Hokkaido University for their kind advice on the picosecond single-photon-counting apparatus. This work was partially supported by The Kawakami Memorial Foundation and a Grant-in-Aid for Scientific Research on Priority Areas, New Functionality Materials—Design, Preparation and Control (No. 63604561), from the Ministry of Education, Science and Culture of Japan.

References and Notes

(1) Johnson, G. E. *J. Chem. Phys.* **1975**, *62*, 4697.
(2) Itaya, A.; Okamoto, K.; Kusabayashi, S. *Bull. Chem. Soc. Jpn.* **1976**, *49*, 2082.
(3) Johnson, G. E. *J. Chem. Phys.* **1975**, *63*, 4047.
(4) Ng, D.; Guillet, J. E. *Macromolecules* **1981**, *14*, 405.
(5) (a) De Schryver, F. C.; Vandendriessche, J.; Toppet, S.; Demeyer, K.; Boens, N. *Macromolecules* **1982**, *15*, 406. (b) Vandendriessche, J.; Palmans, P.; Toppet, S.; Boens, N.; De Schryver, F. C.; Masuhara, H. *J. Am. Chem. Soc.* **1984**, *106*, 8057.
(6) Evers, F.; Kobs, K.; Memming, R.; Terrell, D. R. *J. Am. Chem. Soc.* **1983**, *105*, 5988.
(7) Hoyle, C. E.; Nemzek, T. L.; Mar, A.; Guillet, J. E. *Macromolecules* **1978**, *11*, 429.
(8) (a) Ghiggino, K. P.; Wright, R. D.; Phillips, D. *Eur. Polym. J.* **1978**, *14*, 567. (b) Ghiggino, K. P.; Archibald, D. A.; Thistlethwaite, P. J. *J. Polym. Sci., Polym. Lett. Ed.* **1980**, *18*, 673. (c) Skilton, P. F.; Ghiggino, K. P. *Polym. Photochem.* **1984**, *5*, 179.
(9) Tagawa, S.; Washio, M.; Tabata, Y. *Chem. Phys. Lett.* **1979**, *68*, 276.
(10) Roberts, A. J.; Phillips, D.; Abdul-Rasoul, F. A. M.; Ledwith, A. *J. Chem. Soc., Faraday Trans. 1* **1981**, *77*, 2725.
(11) (a) Masuhara, H.; Tamai, N.; Ikeda, N.; Mataga, N.; Itaya, A.; Okamoto, K.; Kusabayashi, S. *Chem. Phys. Lett.* **1982**, *91*, 113. (b) Itaya, A.; Sasaki, H.; Masuhara, H. *Chem. Phys. Lett.* **1987**, *138*, 231.
(12) Kauffmann, H. F.; Weixelbaumer, W.; Buerbaumer, J.; Schmoltner, A.; Olaj, O. F. *Macromolecules* **1985**, *18*, 104.
(13) Kauffmann, H. F.; Mollay, B.; Weixelbaumer, W.; Buerbaumer, J.; Riegler, M.; Meisterhofer, E.; Aussenegg, F. R. *J. Chem. Phys.* **1986**, *85*, 3566.
(14) Sienicki, K.; Winnik, M. A. *J. Chem. Phys.* **1987**, *87*, 3922.
(15) Hirayama, F. *J. Chem. Phys.* **1965**, *42*, 3163.
(16) (a) Chiellini, E.; Solaro, R.; Ledwith, A. *Makromol. Chem.* **1977**, *178*, 701. (b) Keyanpour-Rad, M.; Ledwith, A.; Johnson, G. E. *Macromolecules* **1980**, *13*, 222.
(17) Houben, J. L.; Natucci, B.; Solaro, R.; Colella, O.; Chiellini, E.; Ledwith, A. *Polymer* **1978**, *19*, 811.
(18) Keyanpour-Rad, M.; Ledwith, A.; Hallam, A.; North, A. M.; Breton, M.; Hoyle, C.; Guillet, J. E. *Macromolecules* **1978**, *11*, 1114.
(19) Chapoy, L. L.; Biddle, D. *J. Polym. Sci., Polym. Lett. Ed.* **1983**, *21*, 621.
(20) Solaro, R.; Galli, G.; Masi, F.; Ledwith, A.; Chiellini, E. *Eur. Polym. J.* **1983**, *19*, 433.
(21) Ito, S.; Yamashita, K.; Yamamoto, M.; Nishijima, Y. *Chem. Phys. Lett.* **1985**, *117*, 171.
(22) Burkhart, R. D.; Lee, O.; Boileau, S.; Boivin, S. *Macromolecules* **1985**, *18*, 1277.
(23) Ito, S.; Takami, K.; Yamamoto, M. *Makromol. Chem., Rapid Commun.* **1989**, *10*, 79.
(24) Buu-Hoi, N. P.; Cagniant, P. *Ber.* **1944**, *77*, 121.
(25) Neugebauer, F. A.; Fischer, H. *Chem. Ber.* **1972**, *105*, 2686.
(26) Okamoto, K.; Yamada, M.; Itaya, A.; Kimura, T.; Kusabayashi, S. *Macromolecules* **1976**, *9*, 645.
(27) Melhuish, W. H. *J. Phys. Chem.* **1961**, *65*, 229.

(28) Yamazaki, I.; Kume, H.; Tamai, N.; Tsuchiya, H.; Oba, K. *Rev. Sci. Instrum.* **1985**, *56*, 1187.
(29) (a) Kanaya, T.; Hatano, Y.; Yamamoto, M.; Nishijima, Y. *Bull. Chem. Soc. Jpn.* **1979**, *52*, 2079. (b) Ito, S.; Yamamoto, M.; Nishijima, Y. *Bull. Chem. Soc. Jpn.* **1982**, *55*, 363.
(30) Ikeda, T.; Lee, B.; Kurihara, S.; Tazuke, S.; Ito, S.; Yamamoto, M. *J. Am. Chem. Soc.* **1988**, *110*, 8299.
(31) (a) Brant, D. A.; Flory, P. J. *J. Am. Chem. Soc.* **1965**, *87*, 2791. (b) Abe, A.; Jernigan, R. L.; Flory, P. J. *J. Am. Chem. Soc.* **1966**, *88*, 631. (c) Yoon, D. Y.; Sundararajan, P. R.; Flory, P. J. *Macromolecules* **1975**, *8*, 776.
(32) Wesson, L. G. *Tables of Electric Dipole Moments*; Technology: Cambridge, 1948.
(33) Szwarc, M. *Carbanions, Living Polymers, and Electron-Transfer Processes*; Interscience: New York, 1968.
(34) Kurahashi, M.; Fukuyo, M.; Shimada, A. *Bull. Chem. Soc. Jpn.* **1969**, *42*, 2174.
(35) Popova, E. G.; Chetkina, L. A. *J. Struct. Chem.* **1979**, *20*, 564.
(36) Sundararajan, P. R. *Macromolecules* **1980**, *13*, 512.
(37) Birks, J. B. *Photophysics of Aromatic Molecules*; Wiley: London, 1970.
(38) Bovey, F. A. *High Resolution NMR of Macromolecules*; Academic: New York, 1972.
(39) Abe, A.; Kobayashi, H.; Kawamura, T.; Date, M.; Uryu, T.; Matsuzaki, K. *Macromolecules* **1988**, *21*, 3414.

Registry No. BCz, 37500-95-1; BEtCz, 51545-40-5; *meso*-BCzPe, 126457-39-4; (±)-BCzPe, 126424-15-5; PBVCz, 120468-30-6; BVCz, 120468-29-3; *tert*-butyl chloride, 507-20-0; bromoethane, 74-96-4; 2,4-bis(tosyloxy)pentane, 35196-66-8; 9-(2-chloroethyl)-3,6-di-*tert*-butylcarbazole, 120484-95-9; carbazole, 86-74-8.

Fluorescence Studies of Coalescence and Film Formation in Poly(methyl methacrylate) Nonaqueous Dispersion Particles[1]

Önder Pekcan[2] and Mitchell A. Winnik*

Department of Chemistry and Erindale College, University of Toronto, Toronto, Ontario, Canada M5S 1A1

Melvin D. Croucher

Xerox Research Centre of Canada, 2660 Speakman Drive, Mississauga, Ontario, Canada L5K 2L1

Received August 3, 1989; Revised Manuscript Received November 15, 1989

ABSTRACT: Poly(methyl methacrylate) [PMMA] particles (d = 1 μm) were prepared by nonaqueous dispersion polymerization. One batch of particles was labeled with phenanthrene [Phe] groups, and a second batch, with anthracene [An]. When mixed, spread as thin films, and then heated above the glass transition temperature of the PMMA, coalescence occurred. Particle fusion was accompanied by increasing amounts of nonradiative energy from Phe* to An. Energy transfer was followed quantitatively by carrying out fluorescence decay measurements on samples quenched to room temperature. The data fit nicely to a Fickian diffusion model and yield values of the diffusion coefficients, D, on the order of 10^{-15} cm^2 s^{-1}. These D values characterize the diffusion of (labeled) polymer molecules across the particle–particle boundary. Since the PMMA in the particles has a broad molecular weight distribution, the D values represent an ensemble average over that distribution.

When dispersions of latex particles are allowed to dry, coalescence occurs to form a continuous polymer film if drying occurs above a certain minimum temperature, called, appropriately, the minimum film-forming temperature [MFT].[3] Coalescence is the essential step in all coating applications of latex-based preparations, and the topic has received extensive attention, particularly by the paint industry. Some traditional concerns have been, for example, the dependence of the MFT on particle composition, size, and morphology.[4,5] Also very important in the case of aqueous latex preparations is an understanding of the forces generated, and their origin, during water evaporation from the coating.[6] These forces must be sufficiently strong to induce deformations in the particle from their original spherical shape to close-packed polyhedra and then to promote fusion into continuous films.

While the issue of molecular diffusion of polymer molecules during coalescence has always been recognized, it is only recently that tools have become available to study this process directly. The fundamental question is, first, to what extent polymer molecules diffuse across the particle boundary during film formation, and, second, how this diffusion depends upon latex composition and structure.

There have been a number of indirect approaches to this question. In transmission electron microscopy [TEM], one can often see the particle boundaries in newly formed films. These have a characteristic hexagonal shape.[7] Since the surface of many latex particles is negatively charged, the interparticle interfaces in the film can be stained for TEM measurements. One curious feature to emerge from the TEM studies is that, in some instances, the particle boundaries eventually disappear,[8] suggesting extensive polymer diffusion across the interface, while in other cases, these particle boundaries persist for weeks and months.[7]

Another approach to the question of latex fusion involves measuring the permeability of the latex films to gasses and vapors. Solvent-cast films are normally continuous and provide a benchmark against which latex films can be compared. Chainey et al.[9] have studied the time evolution of the permeability of latex films. They found that this permeability decreased substantially with time but never reached the same low level obtained in films of the same material prepared by solvent casting. These results were interpreted by assuming that, in the latex

0024-9297/90/2223-2673$02.50/0 © 1990 American Chemical Society